Original paper

Chemical composition and Raman spectroscopy of aerugite, xanthiosite, and a natural analog of $KNi_3(AsO_4)(As_2O_7)$ from Johanngeorgenstadt, Germany

Iwona KORYBSKA-SADŁO*, Adam SZUSZKIEWICZ, Marta PRELL, Piotr GUNIA

Institute of Geological Sciences, University of Wrocław, 50-205 Wrocław, Cybulskiego 30, Poland; e-mail: iwona.korybska-sadlo@uwr.edu.pl

* *Corresponding author*

Aerugite $Ni_{8.5}(AsO_4)_2As^{5+}O_8$ and xanthiosite $Ni_3(AsO_4)_2$, two rare anhydrous arsenates, have been identified in a historic sample from Johanngeorgenstadt, Saxony, Germany. The minerals have been characterized through scanning electron microscopy, electron microprobe analysis and Raman spectroscopy for the first time. They are mostly dark-green (aerugite) to light-green (xanthiosite) fine-grained or microcrystalline crusts on a quartz matrix in association with barite, bunsenite, dolomite, and rooseveltite. Aerugite forms up to 200 μm large pseudo-hexagonal platy crystals, whereas xanthiosite forms short prisms to nearly equant forms, often with indistinct, poorly-developed and rounded faces. The chemical composition of the two minerals can be expressed by the empirical formulas: $(Ni_{7.92}Co_{0.52}Cu_{0.06})_{\Sigma 8.50}(As_{1.00}O_4)_2As_{1.00}O_8$ with traces of Bi (aerugite, mean of 4 analyses, based on 32 oxygens) and $(Ni_{2.85}Co_{0.12}Cu_{0.03})_{\Sigma 3.00}(As_{1.00}O_4)_2$ (xanthiosite, mean of 5 analyses, based on 32 oxygens). The Raman spectra of both minerals lack bands related to OH stretching vibrations and are dominated by antisymmetric ν_3 and symmetric ν_1 As–O vibrations in AsO_4 polyhedra centered at 817, 846 and 886 cm^{-1} in the case of aerugite and at 786, 808, 826 and 843 cm^{-1} in xanthiosite. Bands from stretching vibrations As-O in AsO_4 polyhedra are located at 728 and 735 cm^{-1} in aerugite and are slightly displaced to 726 and 747 cm^{-1} in xanthiosite. The Raman spectrum of aerugite also contains well-defined 692, 675 and 658 cm^{-1} bands due to the stretching mode of NiO_6 octahedra, a broad feature at 576 cm^{-1} probably from a number of modes connected with AsO_6 octahedra. On the other hand, the xanthiosite spectrum displays a number of low-intensity, well-defined bands related to antisymmetric ν_4 and ν_2 symmetric bending vibrations in AsO_4 below 700 cm^{-1} as well as to lattice vibrational modes and Ni-O interactions below 250 cm^{-1}. Locally, the interstices between xanthiosite grains are filled with cryptocrystalline mass with the mean chemical composition of $(K_{0.90}Ba_{0.01})_{\Sigma 0.91}(Ni_{2.86}Co_{0.11}Cu_{0.05})_{\Sigma 3.02}(As_{1.00}O_4)(As_{2.1}O_7)$ with traces of Na (mean of 7 analyses, based on 11 oxygens). The recorded Raman spectrum, with a strongly overlapping xanthiosite-related signal, lacks bands of water molecules or OH groups and contains bands related to the As–O–As vibration modes attributed to pyroarsenate As_2O_7 groups. Although it was impossible to obtain more detailed data on crystal structure, we suggest this is the first reported natural occurrence of $KNi_3(AsO_4)(As_2O_7)$ phase.

Keywords: aerugite, xanthiosite, $KNi_3(AsO_4)(As_2O_7)$, arsenates, chemistry, Raman spectroscopy
Received: 28 March 2022; accepted: 14 October 2022; handling editor: J. Plášil

1. Introduction

Over the last decades, Raman spectroscopy has been widely used in mineral studies and has proven its potential as a reliable and fast technique to provide a structural fingerprint for the characterization and identification of mineral species (Nasdala et al. 2004). Being a non-destructive method, Raman spectroscopy is found particularly useful in studying rare and valuable objects such as historic mineral and rock samples stored in museums and private collections. Such collections are not only a part of scientific and cultural world heritage but also represent a highly valuable base for various didactic and scientific purposes. However, historic specimens sometimes lack precise mineral identifications. They can be misidentified, named, and classified according to outdated classification systems or simply have their original descriptions lost or erroneously associated with samples. Such samples need re-examination by means of non-invasive methods, and in this context, Raman spectroscopy is a very effective tool (Barone et al. 2015, 2016; Mazzoleni et al. 2016). However, although a great number of Raman spectra have been published and several projects aiming at building open-access databases have been launched, the applicability of Raman spectroscopy for fast mineral identification is still hampered by the lack of reference Raman spectra, especially in the case of very rare mineral species.

In this study, we present the results of the investigations of an enigmatic mineral sample of anhydrous nickel arsenates from a historical collection of the Mineralogical Museum of the University of Wrocław, Poland. The origi-

nal aim of our research was to identify minerals in the sample using micro-Raman spectroscopy. The obtained Raman spectra suggested the presence of three distinct mineral species. However, the spectra did not match the reference spectra in the available databases. Therefore, we also applied scanning electron microscopy, X-ray diffraction and electron microprobe, which allowed the identification and detailed characterization of aerugite and xanthiosite, very rare nickel arsenates. To our best knowledge, this is the first study of these minerals by Raman spectroscopy. We also present the first description of a natural analog of a synthetic $KNi_3(AsO_4)(As_2O_7)$ phase that co-occurs with xanthiosite.

Aerugite, $Ni_{8.5}(AsO_4)_2As^{5+}O_8$ and xanthiosite, $Ni_3(AsO_4)_2$ are very rare anhydrous nickel arsenates described for the first time in 1858 (Bergemann 1858). They occur as secondary minerals in an oxidized zone of nickel arsenic deposits. Johanngeorgenstadt, Germany, the type locality for these two minerals, is the only known locality where they co-occur. The identification of aerugite and xanthiosite in the material from the South Terras mine, Cornwall, UK (Davis et al. 1965) is now believed to be erroneous (Roberts et al. 2001).

Aerugite forms dark grass-green, blue-green and pale brown, very fine-grained to cryptocrystalline masses and encrustations. Euhedral crystals up to 1 mm in size are very rare (Roberts et al. 2001). Cleavage is not observed and hardness is 4 on the Mohs scale. Aerugite is trigonal, $R\bar{3}m$ space-group, and has unit cell parameters: a = 5.951, c = 27.568 Å, Z = 3, V = 845.50 Å^3 (Fleet and Barbier 1989). The crystalline structure of aerugite is composed of three layers parallel to [111]. Two are built of NiO_6 octahedra and AsO_4 tetrahedra, and one of NiO_6 and AsO_6 octahedra. In the last layer, only 5/6 of the NiO_6 octahedra are occupied in order to maintain electrostatic balance. It is worth noticing that aerugite is the only naturally occurring mineral with octahedrally coordinated As (Fleet and Barbier 1989).

Xanthiosite occurs as golden yellow or light green powdery aggregates and very fine-grained encrustations. Very rare euhedral crystals, up to 0.5 mm large, have also been noted (Roberts et al. 2001). It has a hardness of 4 on the Mohs scale. Xanthiosite is monoclinic, $P2_1/c$ space group, and has unit cell parameters: a = 5.764, b = 9.559, c = 10.194 Å, β = 92.95°, and V = 560.9 Å^3. Synthetic orthorhombic polymorph, *Cmca* space group, with unit-cell parameters: a = 5.943, b = 11.263, c = 8.164 Å, V = 546.5 Å^3 is also known (Barbier and Frampton 1991). The crystal structure of xanthiosite is similar to the structure of olivines and is cation-deficient. The three-dimensional framework structure is built of NiO_6 octahedra and AsO_4 tetrahedra arranged in layers stacked in the *b*-axis direction, where Ni octahedra are connected by edges and corners with the As tetrahedra (Barbier and Frampton 1991). However, compared to A_2BO_4 stoichiometry in the case of olivines, the charge balance is maintained by 1/4 of the available octahedral sites being vacant. As a result, the stoichiometry in xanthiosite changes to $Ni_{1.5}AsO_4$.

The aerugite- and xanthiosite-bearing specimen studied by us is stored in the Mineralogical Museum of the University of Wrocław, Poland, under the catalog number MMUWr II-15889. The original label indicates that it was obtained from the Krantz company in 1871 by Professor Martin Websky, who donated the specimen to the Mineralogical Museum of the University of Wrocław (then Breslau). The label informs that the specimen comes from Johanngeorgenstadt, Saxony, Germany and contains anhydrous nickel arsenates with the chemical formulas: $Ni_5As_2O_{10}$ and $Ni_3As_2O_8$ (Fig. 1). However, no specific mineral names are given. Therefore, we assume that no phase identification study has been performed on the sample so far. There is also no information on whether the chemical formulas were achieved by the investigation of material from exactly this specimen or from other similar samples. The second option seems more probable, considering that in the mid-19th century, classical methods of wet chemical analysis required the extraction of nonnegligible amounts of material and that our specimen did not show any signs of such activities. On the label, there is an additional short reference to the publication from 1858 (Bergemann 1858) with chemical analyses of similar nickel arsenates from Johanngeorgenstadt.

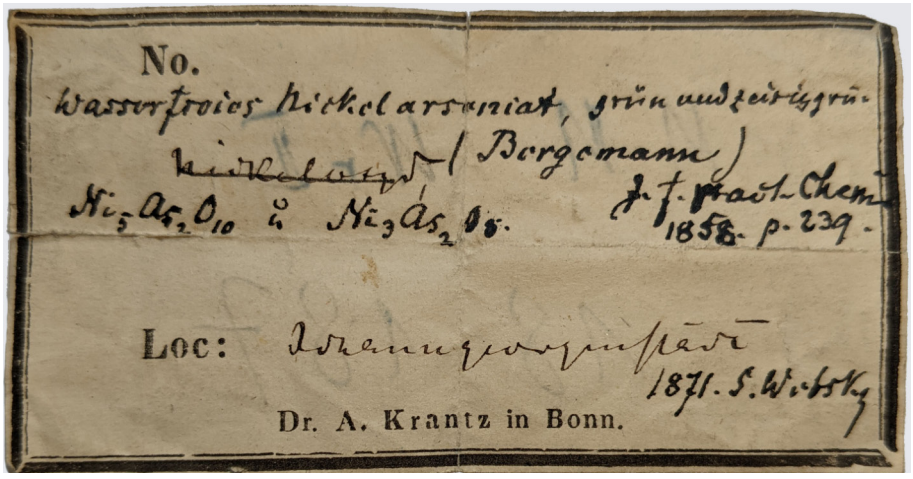

Fig. 1 The original label of the studied sample MMUWr II-15889, stored in the Mineralogical Museum of the University of Wrocław, Poland.

The investigated specimen measures ca. 18 × 25 × 18 mm and consists of fine-grained quartz mostly covered by very fine-grained to cryptocrystalline dark green to light green crust. The crust is porous in some parts, with submicroscopic to millimeter-seized pores, while it appears nearly massive in other parts. A few larger and mostly elongated cavities, up to 0.5 × 8 mm, are lined with well-shaped tiny crystals (Fig. 2).

The overall megascopic appearance of the specimen very closely resembles aerugite- and xanthiosite-bearing historical samples from Johanngeorgenstadt studied by other researchers (Bergemann 1858; Roberts et al. 2001, 2004; Kampf et al. 2020). It seems that it is a fragment of a larger historical finding that pieces are now dispersed in various private and museum mineral collections. Thus, it can be inferred that the MMUWr II-15889 specimen is a part of the exotic minerals assemblage that includes aerugite, bunsenite, johanngeorgenstadtite, niasite, paganoite, petewilliamsite, quartz, rooseveltite and xanthiosite. This assemblage formed from primary nickeline ore under relatively dry and oxidizing conditions and is unique for Johanngeorgenstadt (Roberts et al. 2001, 2004; Kampf et al. 2020). Nickeline veinlets rimmed by native bismuth were also observed in some samples containing petewilliamsite and paganoite (Roberts et al. 2001, 2004). Johanngeorgenstadt mining district is a famous location that has yielded a great number of mineral species related to the mining of silver-nickel-cobalt-uranium ore. Mining in this location dates back to the 16th century and lasted until 1958 when the last uranium mine was closed. Kampf et al. (2020) suggest that the assemblage containing anhydrous Ni arsenates, unique to Johanngeorgenstadt, was probably extracted from the local mines in the 19th century during the reopening of older excavations. They also mention a former mining practice of using fire when extracting a deposit. According to these authors, this firesetting technique may have contributed to the formation of this anhydrous supergene mineral assemblage. This mining practice has been described in detail by Weisgerber and Willies (2000). According to this publication, such wood fire can exceed 700 °C. The temperature was found sufficient to crystallize a synthetic equivalent of niasite (Barbier 1999).

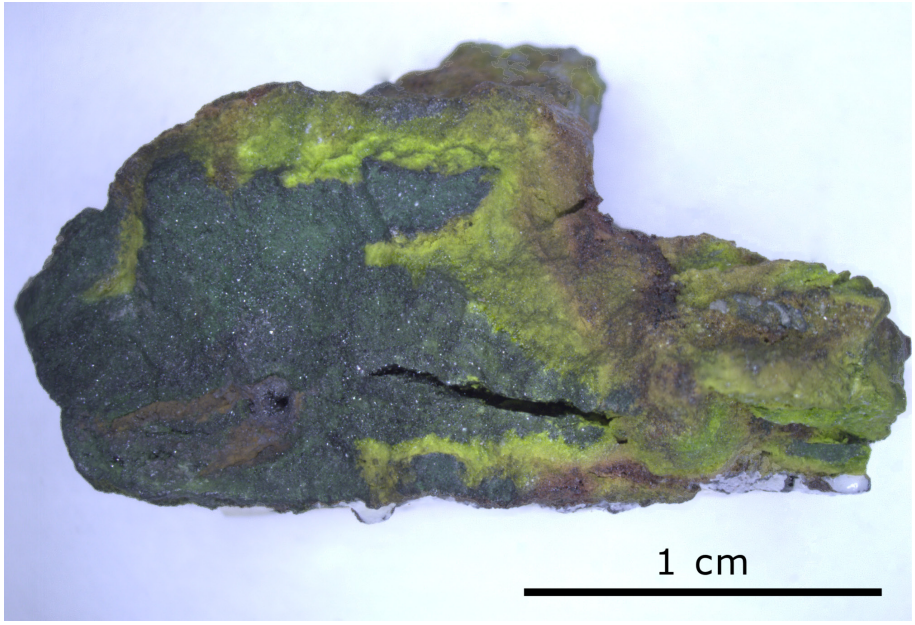

Fig. 2 A research sample MMUWr II-15889 with dark green aerugite and light green xanthiosite.

2. Methods

The MMUWr II-15889 specimen was gently cleaned with a soft brush and thoroughly studied under the binocular and by scanning electron microscopy in low vacuum mode using the Jeol JSM-IT500LA equipped with an Energy Dispersive Spectrometer (SEM-EDS) at the Institute of Geological Sciences, University of Wrocław, Poland. In addition, semi-quantitative standardless chemical analyses by EDS were carried out for preliminary mineral identification.

A small representative fragment was extracted from the specimen to prepare a powder sample for X-ray diffraction (XRD) because the analyzed minerals were too fine-grained for single-crystal X-ray studies. XRD patterns were collected at the Institute of Geological Sciences, University of Wroclaw, Poland, using a Brucker D8 Advance diffractometer. The measurements were conducted with CuK_α radiation source in the range of 2Θ angles between 3° and 75°, with a time/step size of 0.4°, operating at 40 kV and 40 mA. The total measurement time of each scan was 48 min. The Diffrac Eva V 5.0 Suite software supplied by Bruker Corporation was applied to interpret obtained results.

After preparing the powder, the remnants of the sub-sample were mounted in epoxy resin into a 1-inch cylindrical disc, polished and coated with carbon. The disc was used for quantitative chemical point analyses carried out at the Inter-Institute Analytical Complex for Minerals and Synthetic Substances, University of Warsaw, Poland using a CAMECA SX100 electron microprobe analyzer (EMPA) operating in wavelength-dispersive spectroscopy mode. An accelerating voltage of 15kV, beam current of 10nA, beam size 5μm, and a

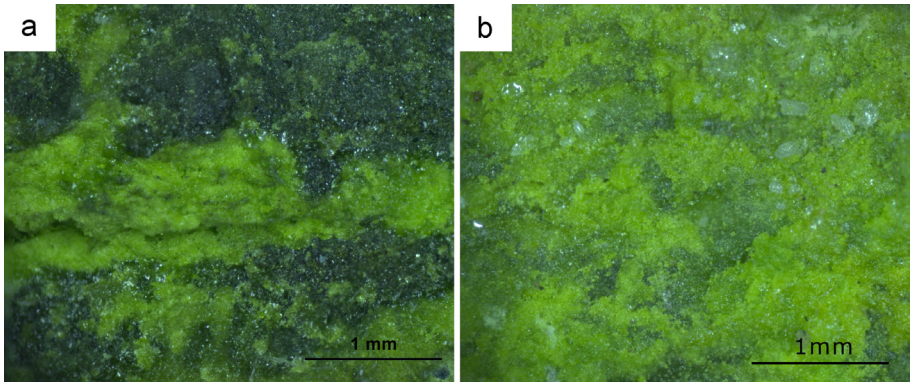

Fig. 3 Close-up image of crystals on MMUWr II-15889 specimen: **a** – fine-grained crust built of aerugite (dark green) and xanthiosite (light green); **b** – probably rooseveltite crystals (colorless) on xanthiosite (light green).

peak counting time of 10s were applied. In the case of $KNi_3(AsO_4)(As_2O_7)$, the operating conditions were: an accelerating voltage of 10kV, a beam current of 8nA, and a beam size of 2 μm.

The following standards were used: Na – albite, K – orthoclase, Ca – diopside, Bi – Bi_2Te_3, As – GaAs, Ba – barite, Co – CoO, Ni – NiO, Cu – cuprite, Ti – rutile, P – $LaPO_4$, Sr – celestine. Data reduction was made using the method of Pouchou and Pichoir (1985).

Micro-Raman analyses were carried out on the whole specimen and on the disc after the removal of the carbon coating. The measurements were performed at the Institute of Geological Sciences, University of Wrocław, Poland, using the Renishaw inVia Qontor confocal Raman microscope equipped with a LEICA DM2700M 50× lens with a working distance of 0.5 mm (numerical aperture 0.75). A diode 532 nm laser was used for excitation with an emission line of a 5 mW power on the sample and a 20 s exposure time. To disperse the light, a grating with 1800 l/mm was used, and a Renishaw Centrus 1HW905 charge-coupled device (CCD) detector with 1040 × 256 pixels and a distance between pixel center 26 × 26 μm was employed to detect the scattered Raman light with a spectral resolution of 1.49 cm^{-1}. The Raman spectra were recorded in 50–4000 cm^{-1} range. Collected data were processed using the software Spectragryph 1.2.15.

3. Results and discussion

3.1. Mineral assemblage – optical studies, Scanning Electron Microscopy (SEM-EDS), X-ray Diffraction (XRD)

Binocular and SEM-EDS studies confirm that secondary minerals dark-green to light-green crust is essentially built of two distinct nickel arsenates (Figs 3a, 3b). The dark-green to very dark-green portions are aggregates dominated by aerugite, while the light-green ones mainly consist of xanthiosite. On the other side of the sample, xanthiosite is more yellow: yellow-brown, orange-red to brownish purple. In addition, several short prismatic euhedral crystals, ca. 0.1 mm long, scattered on one side of the sample, are colorless to white with an adamantine luster. They have been tentatively identified as rooseveltite (Fig. 3b). In the largest cavities, tiny crystals of bunsenite and a few submicroscopic grains of dolomite and barite are present.

Back-scattered electron (BSE) imaging using SEM-EDS reveals that aerugite forms euhedral to subhedral tabular crystals, up to 200 μm in size. The crystals are dominated by {0001} faces, typically with pseudo-hexagonal appearance, sometimes with visible growth steps (Figs 4a, 4b). Rhombohedral faces are subordinate and other crystallographic forms are hard to define due to small crystal sizes.

Xanthiosite occurs as euhedral and subhedral short stubby prisms to nearly equant forms, approximately 2–20 μm in size (Figs 5a, 5b). Some crystals are bounded by well-defined faces, edges and corners. Others show a peculiar morphology that results from a complex combination of various crystal-

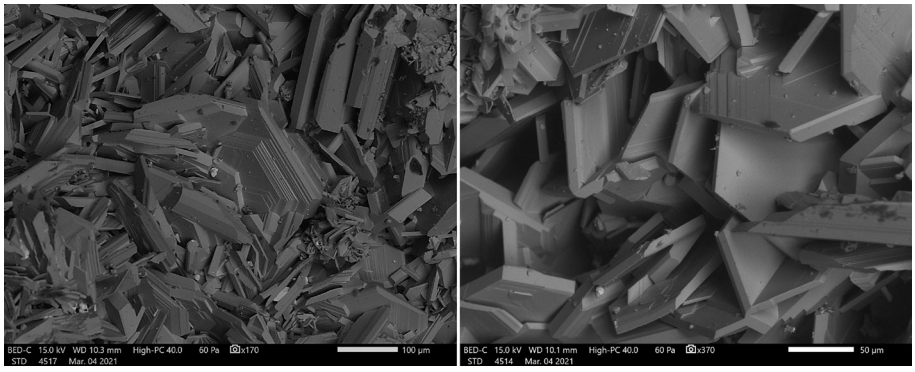

Fig. 4 Back-scattered electron image of aerugite crystals on MMUWr II-15889 specimen: **a** – well-formed crystals of aerugite; **b** – a close-up image of euhedral aerugite crystals.

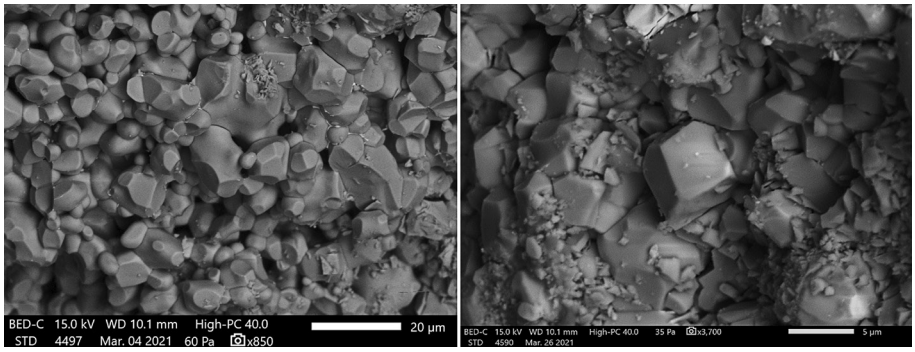

Fig. 5 Back-scattered electron image of crystals of xanthiosite from MMUWr II-15889 specimen: **a** – euhedral and subhedral short stubby prisms of crystals of xanthiosite; **b** – well-formed xanthiosite crystal.

lographic forms whose accurate identification is beyond the current study and would require a single-crystal analysis, e.g., optical goniometry (Figs 5a, 5b), indistinct edges, and ill-developed or rounded faces. In extreme cases, the crystals have a spherulite-like appearance. This morphology may be a result of surface dissolution or growth peculiarities. It is noteworthy that petewilliamsite, a Ni–Co arsenate associated with xanthiosite and aerugite from Johanngeorgenstadt, was also found to possess rounded crystal faces (Roberts et al. 2004).

In a fragment prepared as a polished sample for EMPA analyses, xanthiosite crystals are embedded in a cryptocrystalline matrix (Fig. 6b). Low resistance to polishing than xanthiosite suggests a hardness close to 2–3 on the Mohs scale. In back-scattered electron imaging, no zoning is noticeable and semi-quantitative EDS analyses revealed it is a K and Ni arsenate with small amounts of Ba, Co, and Cu. This mineral has not been observed by optical studies of the entire specimen.

X-ray diffraction patterns were obtained for two powdered samples. One was prepared from a fragment of mineral crust with dark green color and the other was of light green color. The results (Figs 7, 8) conform to the reference X-ray patterns for aerugite and xanthiosite, respectively (PDF 04-009-2302 and PDF 04-016-0062 reference records) in the PDF 4+2022 ICDD database. However, the powder samples are polymineral mixtures and reflections from aerugite and xanthiosite are strongly overlapped by other accompanying phases. As a result, the obtained diffraction patterns could not be indexed and used for unit-cell parameter refinements. It was impossible to obtain the K- and Ni-arsenate sample for the X-ray studies.

3.2. Chemical compositions – Electron Microprobe (EMPA)

Chemical compositions were measured by EMPA in four and five spots on different aerugite and xanthiosite crystals, respectively (Figs 6a, 6b). The analytical results are presented in Tabs 1 and 2, along with the ideal compositions. Other elements, such as Na, K, Ca, Ba, Sr, Ti, and P were sought but not detected. The calculated empirical formulas based on 32 O atoms per formula unit (*apfu*) are $(Ni_{15.85}Co_{1.03}Cu_{0.12}Bi_{0.01})_{\Sigma 17.01}As_{6.00}O_{32}$ for aerugite and $(Ni_{11.39}Co_{0.48}Cu_{0.12})_{\Sigma 11.99}As_{8.00}O_{32}$ for xanthiosite, which corresponds to $(Ni_{7.92}Co_{0.52}Cu_{0.06})_{\Sigma 8.50}(As_{1.00}O_4)_2As_{1.00}O_8$ and $(Ni_{2.85}Co_{0.12}Cu_{0.03})_{\Sigma 3.00}(As_{1.00}O_4)_2$, respectively. The total contents are close to 100 wt. % of the measured elements and little variation of the chemical compositions indicate that both minerals are anhydrous and chemically relatively homogeneous. The empirical formulas closely match the ideal ones as they concern the number of cations and the ratio between As and Ni + Co + Cu.

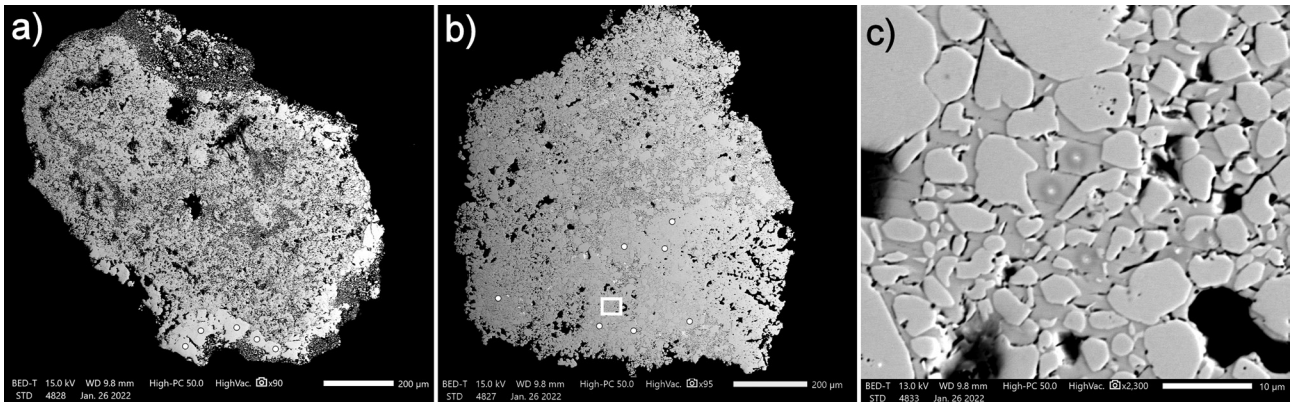

Fig. 6 Back-scattered electron image on MMUWr II-15889 specimen with marked EMPA analytical spots: **a** – image of aerugite dominated fragment; **b** – image of xanthiosite dominated fragment with a marked position of 6c image; **c** – image of xanthiosite embedded in a cryptocrystalline mass of $KNi_3(AsO_4)(As_2O_7)$ with craters due to the damage from the EMPA electron beam.

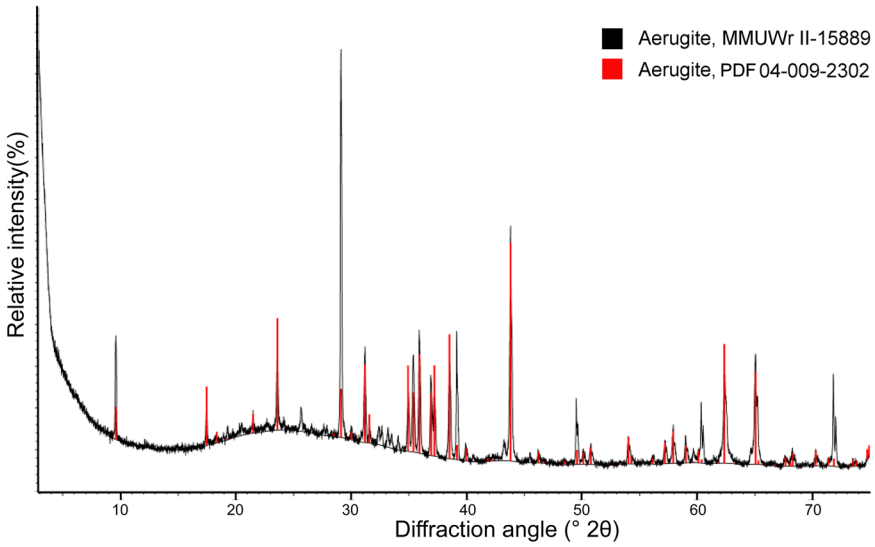

Fig. 7 X-ray diffraction pattern of aerugite from MMUWr II-15889 specimen compared with the reference pattern from PDF 4+2022 ICDD database.

In both minerals, the homovalent substitutions of Co and Cu for Ni are rather limited, being responsible for a few % in the case of Co and up to 1 % in the case of Cu of the Ni-dominated site occupancy. In aerugite, the amount of 15.70–16.22 *apfu* Ni approaches the ideal amount of 17 *apfu*, with the Co and Cu admixtures varying from 0.52 to 1.32 *apfu* and from 0.09 to 0.15 *apfu*, respectively. In xanthiosite, the content of Ni varies from 11.19 to 11.77 *apfu*, also close to the ideal amount of 12 *apfu*. The contents of Co and Cu are 0.33–0.76 *apfu* and 0.08–0.19 *apfu*, respectively. To our best knowledge, there is practically no comparative material published on EMPA chemical analyses of these two minerals. The original analyses of Bergemann (1858), obtained by wet chemical methods and therefore susceptible to contamination by mineral impurities, give (in wt. %) 0.14 P_2O_5,

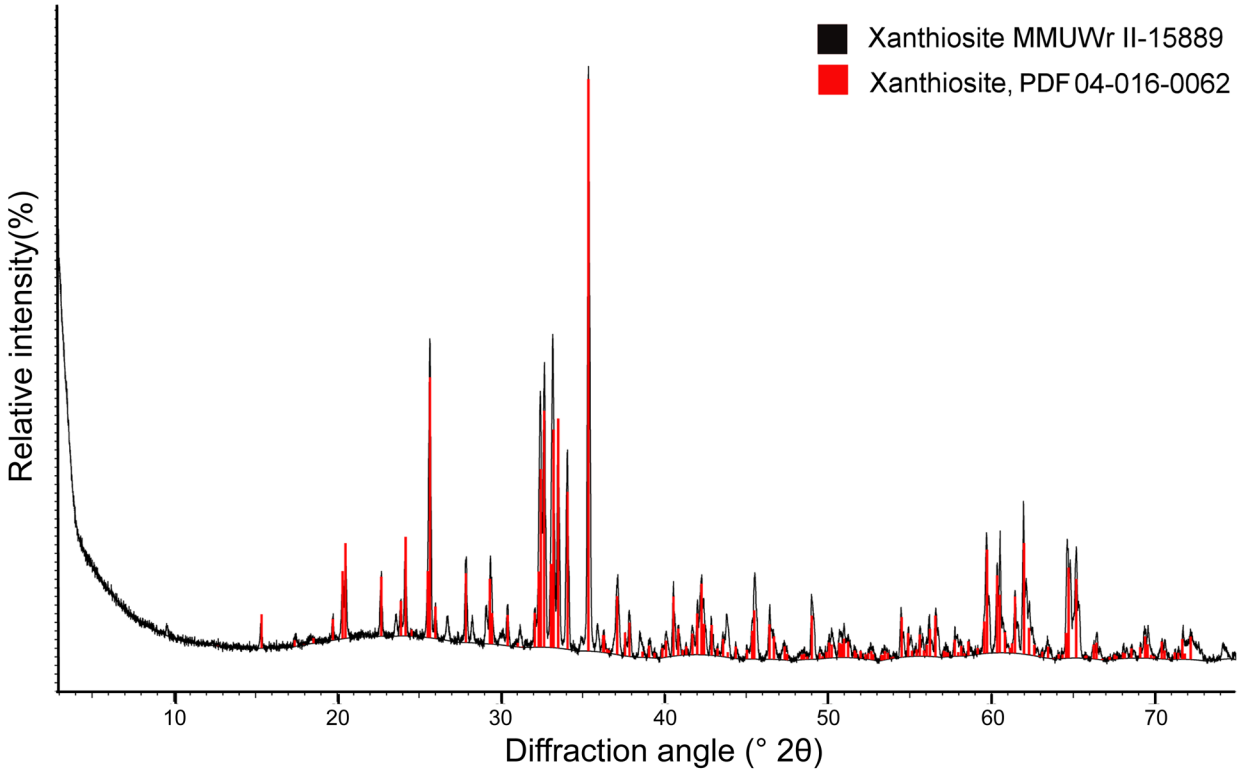

Fig. 8 X-ray diffraction pattern of xanthiosite from MMUWr II-15889 specimen compared with the reference pattern from PDF 4+2022 ICDD database.

36.57 As_2O_5, 0.24 Bi_2O_3, 0.54 CoO, 62.07 NiO, 0.34 CuO, and traces of Fe_2O_3 for aerugite and 50.53 As_2O_5, 0.62 Bi_2O_3, 0.21 CoO, 48.24 NiO, and 0.57 CuO for xanthiosite. For both minerals, they show one order of magnitude lower contents of CoO and very similar amounts of CuO compared to our results (Tabs 1, 2). It is, however, not clear whether the difference in CoO concentrations results from some systematic discrepancy between different analytical methods or really documents variation of Co-enrichment in aerugite and xanthiosite from Johanngeorgenstadt.

Tab. 1 Mean chemical compositions of aerugite from MMUWr II-15889 specimen. Theoretical compositions calculated from ideal formulas are given for comparison. Number of analyses are given in parenthesis.

	#28	#29	#30	#34	Mean (4)	S.D.	Ideal
NiO	60.30	60.25	60.90	61.98	60.86	0.80	64.81
CoO	5.10	4.82	3.98	2.01	3.97	1.39	
CuO	0.46	0.52	0.60	0.37	0.49	0.10	
Bi_2O_3	0.00	0.00	0.00	0.39	0.10	0.19	
As_2O_5	35.13	35.24	35.79	35.56	35.43	0.30	35.19
Total	100.99	100.83	101.28	100.31	100.85		100.00
Atoms per formula unit based on 32 O							
Ni	15.70	15.70	15.77	16.22	15.85	0.25	17
Co	1.32	1.25	1.03	0.52	1.03	0.36	
Cu	0.11	0.13	0.15	0.09	0.12	0.02	
Bi	–	–	–	0.03	0.01	0.02	
As	5.95	5.97	6.02	6.05	6.00	0.05	6
Total	23.08	23.05	22.97	22.91	23.00		

#n = label of the analysis; S.D. = standard deviation; b.d.l. = below the detection limit.

Compared to our results, even higher contents of Co and Cu (except for niasite) were found in other anhydrous arsenates from a very similar mineral assemblage from Johanngeorgenstadt: niasite and johanngeorgenstadtite $(Ni,Co)_{4.5}(AsO_4)_3$, paganoite $NiBiAsO_5$, and petewilliamsite $(Ni,Co)_{30}(As_2O_7)_{15}$ (Kampf et al. 2000; Roberts et al. 2001; 2004). Thus, it seems that the substitution $NiCo_{-1}$ is a characteristic feature of the studied assemblage of arsenate minerals. The Co source is unknown, but it has been suggested that primary nickeline can be Co-enriched (Roberts et al. 2004). Cobalt analogs, $Co_8As_3O_{16}$ and $Co_3(AsO_4)_2$, of aerugite and xanthiosite, respectively, have been synthesized (Krishnamachari and Calvo 1970b, 1970a), although the extent of potential solid solutions between the Ni- and Co-dominated phases have not been studied.

The presence of a trace amount of 0.10 wt. % Bi_2O_3 in the aerugite is comparable to the analysis of aerugite by Bergemann (1858). It is worth mentioning that several crystals of rooseveltite $Bi[AsO_4]$ have been tentatively identified in the studied sample. No other Bi minerals were found. However, native bismuth overgrowing nickeline veinlets was found in a very similar specimen that yielded niasite and johanngeorgenstadtite (Roberts et al. 2001). Therefore, Bi was present in the crystallization environment and we assume it is a structural component of the investigated aerugite. We treated Bi as an element substituting octahedrally coordinated Ni. However, Bi could also be assigned to AsO_6 octahedra or AsO_4 tetrahedra as a cation substituting for As.

Performing EMPA analyses of K and Ni arsenate that builds cryptocrystalline mass, filling the interstices between the xanthiosite crystals (Figs 6b, 6c) was a challenging task. Test analyses using a focused beam with an accelerating voltage of 15 kV and beam current of 10 nA caused significant sample damage. On the other hand, the analytical beam diameter of 5 μm could not be used because homogeneous areas built of the mineral were too small. Therefore, in order to find a compromise between the accuracy of the analyses and the spatial resolution, the 2-μm beam, accelerating voltage of 10 kV, and beam current of 8 nA were applied. Nevertheless, some damage from the electron beam was still observed (Fig. 6c). Some analyses also showed abnormally high concentrations of NiO, implying contamination from the neighbor-

Tab. 2 Mean chemical compositions of xanthiosite from MMUWr II-15889 specimen. Theoretical compositions calculated from ideal formulas are given for comparison. Number of analyses are given in parenthesis.

	#22	#23	#24	#25	#26	Mean (5)	S.D.	Ideal
NiO	47.67	47.10	45.98	45.98	48.57	47.06	1.12	49.36
CoO	1.74	1.92	3.11	1.68	1.38	1.97	0.67	
CuO	0.34	0.40	0.82	0.55	0.62	0.55	0.19	
Bi_2O_3	b.d.l.	b.d.l.	b.d.l.	b.d.l.	b.d.l.	b.d.l.		
As_2O_5	51.45	51.34	50.22	51.10	50.16	50.85	0.62	50.64
Total	101.20	100.77	100.13	99.31	100.74	100.43		100.00
Atoms per formula unit based on 32 O								
Ni	11.44	11.35	11.19	11.21	11.77	11.39	0.23	12
Co	0.42	0.46	0.76	0.41	0.33	0.48	0.16	
Cu	0.08	0.09	0.19	0.13	0.14	0.12	0.04	
Bi	–	–	–	–	–	b.d.l.		
As	8.03	8.04	7.95	8.10	7.90	8.00	0.08	8
Total	19.96	19.94	20.08	19.85	20.15	20.00		

#n = label of the analysis; S.D. = standard deviation; b.d.l. = below the detection limit.

Tab. 3 Chemical composition of cryptocrystalline mass associated with xanthiosite from MMUWr II-15889 specimen. The formula was calculated on the basis of 11 oxygens. Mean composition is calculated with a number of analyses given in parenthesis. The calculated ideal composition of $KNi_3(AsO_4)(As_2O_7)$ phase is given for comparison.

	#9	#11	#12	#13	#14	#17	#21	Mean (7)	S.D.	Ideal
K_2O	6.54	6.75	7.44	7.32	6.43	7.35	6.26	6.87	0.49	7.65
Na_2O	b.d.l.	b.d.l.	b.d.l.	b.d.l.	b.d.l.	0.12	b.d.l.	0.02	0.04	
BaO	0.26	0.26	0.24	0.36	0.28	0.27	0.33	0.28	0.04	
NiO	34.71	34.64	33.88	34.66	34.13	35.74	34.65	34.63	0.58	36.38
CoO	1.13	1.62	1.90	1.43	1.07	0.96	1.28	1.34	0.33	
CuO	0.41	0.44	0.80	0.64	0.77	0.63	0.54	0.60	0.15	
As_2O_5	56.04	56.15	56.44	55.74	55.62	56.33	55.82	56.02	0.31	55.97
Total	99.09	99.86	100.69	100.15	98.30	101.39	98.88	99.76		100.00
K	0.861	0.882	0.967	0.959	0.853	0.951	0.826	0.900		1
Na	–	–	–	–	–	0.006	–	0.001		
Ba	0.011	0.010	0.010	0.014	0.011	0.011	0.014	0.011		
Ni	2.879	2.857	2.776	2.862	2.854	2.914	2.882	2.861		3
Co	0.094	0.133	0.155	0.117	0.089	0.078	0.106	0.110		
Cu	0.032	0.034	0.061	0.049	0.060	0.049	0.042	0.047		
As	3.022	3.010	3.006	2.991	3.023	2.985	3.017	3.008		3
Total	6.898	6.927	6.975	6.993	6.892	6.992	6.887	6.938		7
K+Na+Ba	0.871	0.893	0.977	0.973	0.864	0.967	0.840	0.913		
Ni+Co+Cu	3.005	3.024	2.992	3.029	3.004	3.040	3.030	3.018		
Positive charges	22.000	22.000	22.000	22.000	22.000	21.983	22.000	21.998		

#n = label of the analysis; S.D. = standard deviation; b.d.l. = below the detection limit.

ing xanthiosite grains. A few analyses yielded very low analytical totals resulting from the microporosity of the analyzed cryptocrystalline aggregates. Such results have been rejected from further calculations. Seven relatively good-quality measurements gave coherent chemical compositions, suggesting that the cryptocrystalline mass is composed of a single mineral species rather than a mixture of minerals. The results along with the calculated mean composition, are shown in Tab. 3. They suggest an anhydrous arsenate of the K_2O–NiO–As_2O_5 system with the cation ratio of K + Na + Ba : Ni + Co + Cu : As close to 1 : 3 : 3. A mineral with such stoichiometry is not known. However, synthetic arsenates, such as $KNiAsO_4$, $K_4Ni_7(AsO_4)_6$ and $KNi_3(AsO_4)(As_2O_7)$, have been obtained (Buckley et al. 1988; Smail et al. 1999; Smail and Jouini 2000). The stoichiometry of the investigated mineral closely matches the one of $KNi_3(AsO_4)(As_2O_7)$; therefore, the formula has been calculated based on 11 O *apfu*. The sum of positive charges in the obtained formula is, except for one analysis, equal to the ideal 22. Assuming that K is substituted by small amounts of Ba and traces of Na, the sum of these cations is slightly lower than 1 (0.840–0.977, mean = 0.913). On the other hand, the sum of Ni + Co + Cu, the elements very likely substituting for each other as in the aerugite and xanthiosite, is usually slightly higher than 3 (2.992–3.040, mean = 3.018), and the amount of As cations in the formula oscillates around 3 (2.985–3.023, mean = 3.008). The deviations from the ideal numbers of the cations result probably from polycrystalline nature and microporosity of the analyzed material, as well as alkali loss due to non-optimal analytical conditions. The last phenomenon would lower the content of K + Na + Ba relative to Ni + Co + Cu and As.

All this considered, we believe that the obtained chemical compositions reflect the composition of a mineral with the mean formula: $(K_{0.90}Ba_{0.01})_{\Sigma 0.91}(Ni_{2.86}Co_{0.11}Cu_{0.05})_{\Sigma 3.02}(As_{1.00}O_4)(As_{2.1}O_7)$ containing also traces of Na. Chemically, the mineral is thus a natural analog of synthetic $KNi_3(AsO_4)(As_2O_7)$ substance. However, it is not currently possible to establish unequivocally whether the two phases have the same crystal structure. The cryptocrystalline mode of occurrence of the studied mineral and its low hardness (~3–4 on the Mohs scale) and sensitivity to damage from the EMPA analytical beam are similar to those observed, e.g., in micaceous and clay mineral phases. The extent of substitution of Co (3.6 %) and Cu (1.7 %) for Ni in the studied mineral is comparable to the ones observed in the co-occurring aerugite and xanthiosite. This may suggest that all three minerals formed under similar physicochemical conditions. The small admixture of Ba is consistent with the presence of a few scattered barite crystals noticed in the studied sample.

The present state of knowledge on the anhydrous arsenate assemblage from Johanngeorgenstadt does not allow far-reaching speculations on the origin of the $KNi_3(AsO_4)(As_2O_7)$ mineral. It might be assumed that it formed simultaneously or nearly simultaneously with aerugite and xanthiosite as well as with other anhydrous Ni–Co arsenates from similar samples reported in the literature, such as johanngeorgenstadtite, niasite, paganoite, petewilliamsite, and rooseveltite (Kampf et al. 2020; Roberts et al. 2001, 2004). If, as suggested by Kampf et al. (2020), the

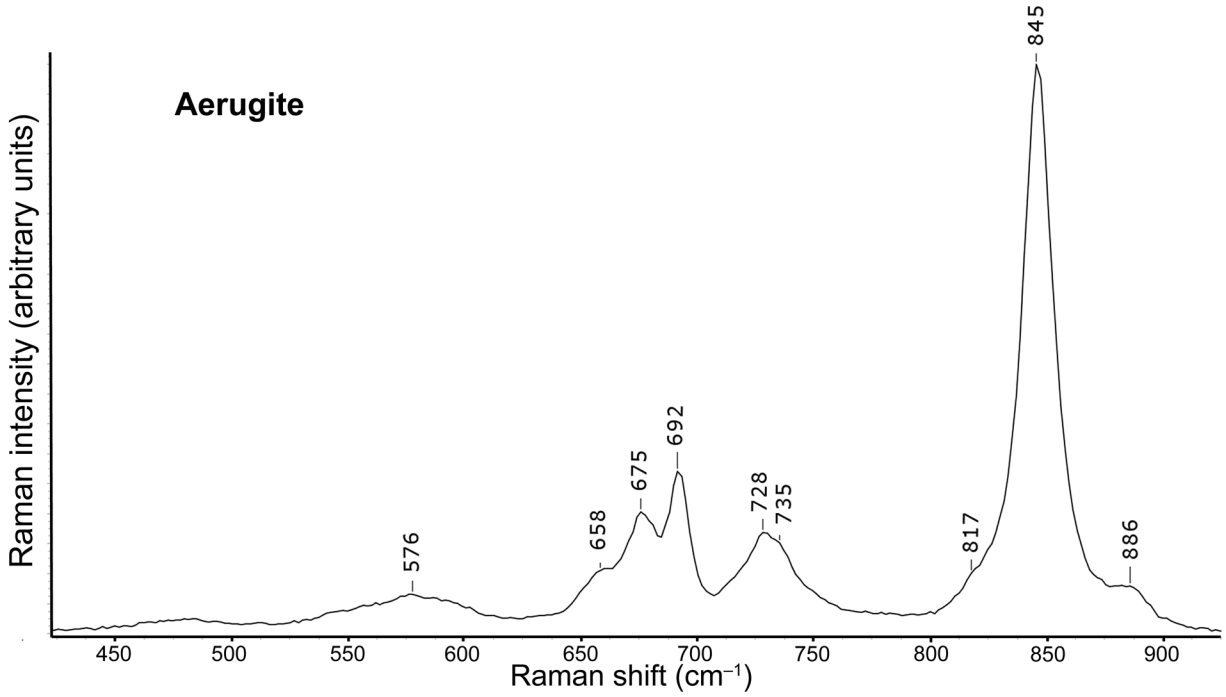

Fig. 9 Raman spectrum of aerugite from MMUWr II-15889 specimen over the 1000–400cm^{-1} spectral range.

firesetting technique used by ancient miners contributed to the formation of this anhydrous arsenates, one might hypothesize that the $KNi_3(AsO_4)(As_2O_7)$ mineral formed from an unknown substrate in the pyrometamorphic process. High-temperature/low-pressure transformation might have led to dehydration and dehydroxylation of the substrate mineral (in the case of the substrate with OH groups or water molecules) and its partial polymerization involving condensation of some of the monoarsenate AsO_4 polyhedra to pyroarsenate As_2O_7 groups.

3.3. Raman spectroscopy

The obtained Raman spectra of aerugite and xanthiosite in the 1000–50 and 1000–400 cm^{-1} spectral range are shown in Figs 9 and 10. It should be noted that both spectra lack bands above 3000 cm^{-1}, in the region of OH stretching vibrations, which confirms the anhydrous composition of the minerals. In both cases, the most prominent features occur in the range from 780 to 850 cm^{-1} and are related to vibration modes within AsO_4 polyhedra (Nakamoto 2009; Kampf et al. 2020). The most intensive bands, assigned to antisymmetric ν_3 and symmetric ν_1 As–O vibrations of the AsO_4 tetrahedra, are observed at 817, 846 and 886 cm^{-1} in aerugite and at 786, 808, 826 and 843 cm^{-1} in xanthiosite. In the range 720–750 cm^{-1}, aerugite also shows bands at 728 and 735 cm^{-1}, while in xanthiosite the bands are shifted to 726 and 747 cm^{-1}. These bands come from stretching vibrations As–O in AsO_4 tetrahedra (Nakamoto 2009). Below 700 cm^{-1}, two groups of bands can be identified in aerugite. Bands at 692, 675 and 658 cm^{-1} are due to the stretching mode of NiO_6 octahedra (Minakshi et al. 2011), and a very broad band at 576 cm^{-1} can result from the superposition of a number of modes connected with AsO_6 octahedra (Bismayer et al. 1986; Losilla et al. 1995). On the other hand, several bands can be identified in the xanthiosite spectrum below 700 cm^{-1}. Most of them are well-defined, although they have low intensities. Several bands in the 600–400 cm^{-1} spectral range can be related to the antisymmetric bending vibrations ν_4 in AsO_4 (Kampf et al. 2020). Symmetric bending ν_2 in AsO_4 is responsible for bands in the 400–250 cm^{-1} range, while lattice vibrational modes and Ni–O interactions give rise to bands below 250 cm^{-1} (Nakamoto 2009; Kampf et al. 2020).

Due to very small homogeneous and monomineral areas built of the $KNi_3(AsO_4)(As_2O_7)$ mineral, we could not achieve a spectrum devoid of the signal from neighboring xanthiosite grains. Therefore, the Raman spectrum in 1000–100 cm^{-1} spectral range shown in Fig. 11 is a superposition of xanthiosite-related and $KNi_3(AsO_4)(As_2O_7)$-related modes. As a consequence, any bands between 850–700 cm^{-1} that might be related to the $KNi_3(AsO_4)(As_2O_7)$ phase cannot be resolved from overlapping bands derived from xanthiosite. Although, in general, the spectrum closely resembles the spectrum of xanthiosite, there are noticeable differences that we attribute solely to the $KNi_3(AsO_4)(As_2O_7)$ phase. The most conspicuous is the presence of bands at 915, 899 and 873 cm^{-1} connected with asymmetric stretching vibra-

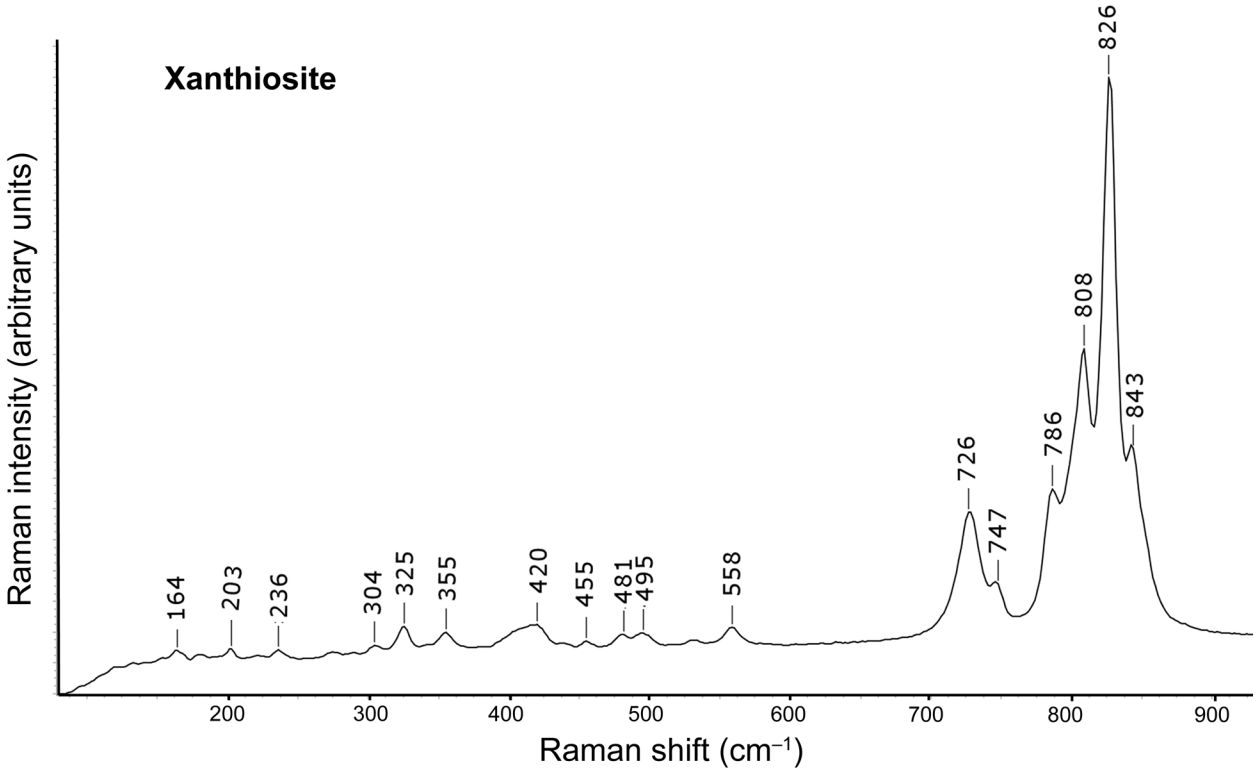

Fig. 10 Raman spectrum of xanthiosite from MMUWr II-15889 specimen over the 1000–100cm^{-1} spectral range.

tions of As–O–As, the band at 586 cm^{-1} connected with symmetric stretching vibrations of As–O–As and bands between 290–220 cm^{-1} connected with bending modes of As–O–As (Baran et al. 2004). The presence of bands related to the As–O–As vibration modes confirms that the mineral contains pyroarsenate As_2O_7 groups. Besides, the absence of bands in a range above 3000 cm^{-1} attests to the anhydrous composition of the mineral.

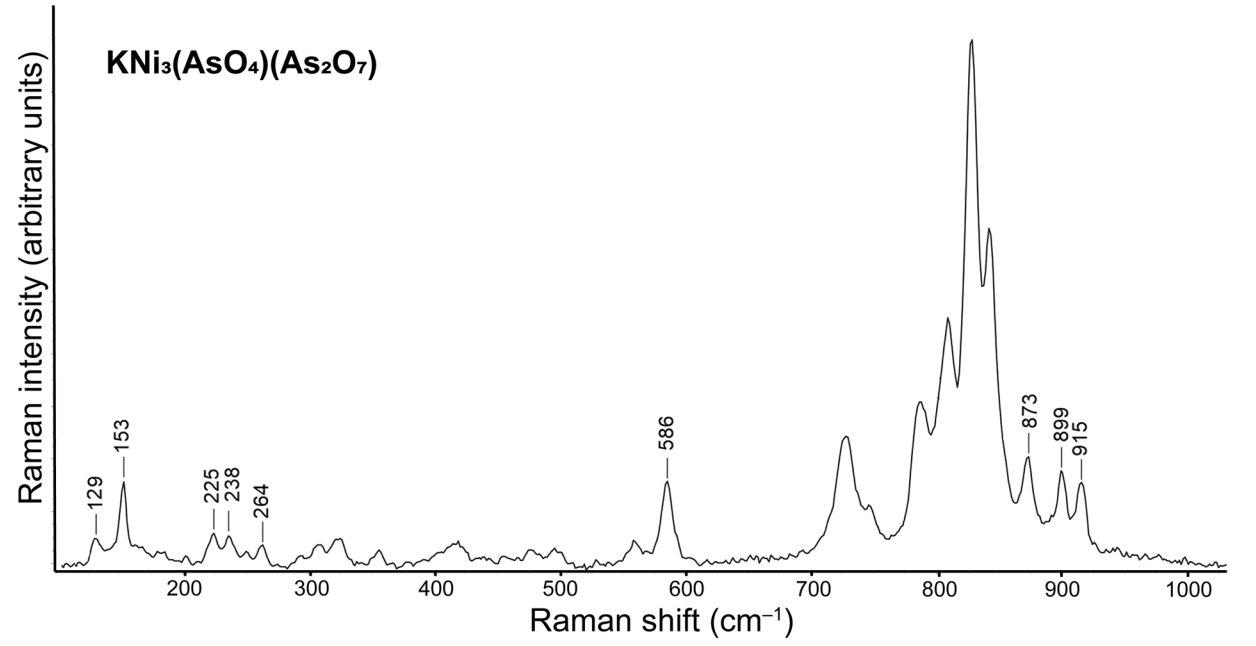

Fig. 11 Raman spectrum over the 1000–100cm^{-1} spectral range of $KNi_3(AsO_4)(As_2O_7)$ from MMUWr II-15889 specimen with overlapping xanthiosite-derived signal. Only the positions of spectral features absent from purely xanthiosite spectra are marked.

4. Conclusions

Aerugite and xanthiosite, two extremely rare anhydrous Ni arsenates, have been identified in an enigmatic historic mineral sample from Johanngeorgenstadt, Germany, housed by the Mineralogical Museum of the University of Wrocław, Poland. The paper presents the first detailed characterization of these minerals through XRD, SEM-EDS, EMPA and Raman spectroscopy methods. The empirical formulas are: $(Ni_{7.92}Co_{0.52}Cu_{0.06})_{\Sigma 8.50}(As_{1.00}O_4)_2As_{1.00}O_8$ with traces of Bi for aerugite and $(Ni_{2.85}Co_{0.12}Cu_{0.03})_{\Sigma 3.00}(As_{1.00}O_4)_2$ for xanthiosite. The obtained Raman spectra can serve as reference standards for these two minerals. The studied sample also contains barite, bunsenite, dolomite, and rooseveltite, as well as, another anhydrous Ni arsenate that occurs as cryptocrystalline filling of interstices between xanthiosite grains. Raman spectroscopy and chemical composition analyses suggest that the mineral is a natural analog of the synthetic $KNi_3(AsO_4)(As_2O_7)$ phase. However, a small amount of the material available for analyses precluded the determination of the crystal structure.

Our observations are consistent with an earlier hypothesis that the ancient firesetting technique used in mining silver–nickel–cobalt–uranium ore at Johanngeorgenstadt could be responsible for the formation of an exotic aerugite- and xanthiosite-bearing mineral assemblage. They also indicate that the substitution $NiCo_{-1}$ is typical of anhydrous Ni arsenates from Johanngeorgenstadt, while the substitution $NiCu_{-1}$ is subordinate and reinforces the supposition that the primary Ni mineralization must have also contained Co and Bi. It should be stressed that discovering the new material bearing this peculiar mineral assemblage is highly unlikely because of a very specific mode of origin. Therefore, future studies of this mineralization will be based on a few historic samples stored in private and museum mineralogical collections. This limits research by destructive methods and increases the importance of non-destructive techniques, such as Raman spectroscopy.

References

Baran E, Enrique J, Weil M (2004) Vibrational Spectra of Cd_2AsO_7. J Raman Spetrosc 35: 178–80

Barbier J (1999) Tetragonal $Ni_{4.35}As_3O_{11.7}(OH)_{0.3}$. Acta Crystallogr C 55, access paper no. IUC9900080

Barbier J, Frampton C (1991) Structures of Orthorhombic and Monoclinic $Ni_3(AsO_4)_2$. Acta Crystallogr B 47: 457–62

Barone G, Bersani D, Jehlička J, Lottici P, Mazzoleni P, Raneri S, Vandenabeele P, Di Giacomo C, Larina G (2015) Nondestructive investigation on the 17–18th centuries Sicilian jewelry collection at the Messina regional museum using mobile Raman equipment. J Raman Spectrosc 46: 989–995

Barone G, Mazzoleni P, Raneri S, Jehlička J, Vandenabeele P, Lottici P, Lamagna G, Manenti A, Bersani D (2016) Raman Investigation of Precious Jewelry Collections Preserved in Paolo Orsi Regional Museum (Siracusa, Sicily) Using Portable Equipment. Appl Spectrosc 70: 1420–1431

Bergemann C (1858) Ueber Einige Nickelerze. J Prakt Chem 75: 239–44

Bismayer U, Salje E, Jansen M, Dreher S (1986) Raman Scattering near the Structural Phase Transition of As_2O_5: Order Parameter Treatment. J Phys C: Solid State 19: 4537–45

Buckley AM, Bramwell ST, Day P, Harrison WTA (1988) The Crystal Structure of Potassium Nickel Arsenate; $KNiAsO_4$. Z Naturforsch B 43(8): 1053–55

Davis RJ, Hey MH, Kingsbury AWG (1965) Xanthiosite and Aerugite. Mineral J 35: 72–83

Fleet ME, Barbier J (1989) Structure of Aerugite ($Ni_{8.5}As_3O_{16}$) and Interrelated Arsenate and Germanate Structural Series. Acta Crystallogr B 45: 201–5

Kampf AR, Nash BP, Plášil J, Smith JB, Feinglos MN (2020) Niasite and Johanngeorgenstadtite, $Ni^{2+}_{4.5}(AsO_4)_3$ Dimorphs from Johanngeorgenstadt, Germany. Eur J Mineral 32: 373–85

Krishnamachari N, Calvo C (1970a) Crystallographic Studies of Cobalt Arsenates I. Crystal Structure of $Co_3(AsO_4)_2$. Can J Chem 48: 881–89

Krishnamachari N, Calvo C (1970b) Crystallographic Studies of Cobalt Arsenates II. Crystal Structure of $Co_8As_3O_{16}$. Can J Chem 48: 3124–31

Losilla ER, Aranda MAG, Ramirez FJ, Bruque S (1995) Crystal Structure and Spectroscopic Characterization of MAs_2O_6 (M = Pb, Ca). Two Simple Salts with AsO_6 Groups. J Phys Chem-US 99: 12975–79

Mazzoleni P, Barone G, Raneri S, Aquilia E, Bersani D, Cirrincione R (2016) Application of micro-Raman spectroscopy for the identification of unclassified minerals preserved in old museum collections. Pliniu 42: 112–124

Minakshi M, Singh P, Appadoo D, Martin DE (2011) Synthesis and Characterization of Olivine $LiNiPO_4$ for Aqueous Rechargeable Battery. Electrochim Acta 56(11): 4356–60

Nakamoto K (2009) Infrared and Raman Spectra of Inorganic and Coordination Compounds. Part A: Theory and Applications in Inorganic Chemistry. 6th Ed Wiley

Nasdala L, Smith DC, Kaindl R, Ziemann MA (2004) Raman spectroscopy: Analytical perspectives in mineralogical research. *In*: Beran A, Libowtzky E (eds) Spectroscopic methods in Mineralogy. EMU Notes in Mineralogy, 6, pp 281–343

Pouchou JL, Pichoir F (1985) "PAP" (φρZ) procedure for improved quantitative microanalysis. In: Armstrong JT (ed) Microbeam Analysis, San Francisco Press pp 104–106

Roberts AC, Burns PC, Gault RA, Criddle AJ, Feinglos MN, Stirling JAR (2001) Paganoite, $NiBi^{3+}As^{5+}O_5$, a New Mineral from Johanngeorgenstadt, Saxony, Germany: Description and Crystal Structure. Eur J Mineral 13: 167–75

Roberts AC, Burns PC, Gault RA, Criddle AJ, Feiglos MN (2004) Petewilliamsite, $(Ni,Co)_{30}(As_2O_7)_{15}$, a New Mineral from Johanngeorgenstadt, Saxony, Germany: Description and Crystal Structure. Mineral Mag 68(2): 231–40

Smail RB, Jouini T (2000) $KNi_3(AsO_4)(As_2O_7)$. Acta Crystallogr C 56(5): 513–14

Smail RB, Driss A, Jouini T (1999) $K_4Ni_7(AsO_4)_6$. Acta Crystallogr C 55(3): 284–86

Weisgerber G, Willies L (2000) The Use of Fire in Prehistoric and Ancient Mining: Firesetting. Paleorient 26(2): 131–49